Iranian Journal of Hydrogen & Fuel Cell 1(2019) 39-58

Iranian Journal of Hydrogen & Fuel Cell

IJHFC

Journal homepage://ijhfc.irost.ir

Green in-situ fabrication of PtW/poly ethylen dioxy thiophene/graphene nanoplates/gas diffusion layer (PtW/ PEDOT /GNP/GDL) electrode and its electrocatalytic property for direct methanol fuel cells application

Maryam Yaldagard*

Department of Chemical Engineering, Urmia University, Iran

Article Information

Article History:

Received:
15 Apr 2019
Received in revised form:
21 July 2019
Accepted:
27 July 2019

Keywords

Direct Methanol Fuel Cell (DMFC)
Galvanostatic Electrodeposition
Graphene Nanoplates
Platinum-Tungsten (PtW) Nanoparticles
Fuel Cell, Poly Ethylen Dioxy Thiophene (PEDOT)

Abstract

In this study nanocomposite films of PtW nanoparticles deposited on a poly ethylen dioxy thiophene/graphene nanoplates/gas diffusion layer (PEDOT/GNP/GDL) electrode are fabricated via an electrochemical route involving a series of electrochemical process. GNPs are in situ reduced on carbon paper covered with 3, 4 ethylen dioxy thiophene during the in situ polymerization of EDOT. PtW nanoparticles 18.57nm in average size are prepared by electrodeposition on the surface of PEDOT/GNP/GDL. Field emission scanning electronic microscopy (FESEM) images showed spongy aggregates of PEDOT densely cover the surface and edges of the GNP layers, implying the existence of a strong interaction between PEDOT and GNP. Based on electrochemical characterization, it was found that the as prepared electrode exhibited comparable activity for the methanol oxidation (MEOH) reaction with respect to commercial Pt/C/GDL based on the traditional sprayed method. A significant reduction in the potential of the CO electro-oxidation peak from 0.92V for Pt/C to 0.75V for the PtW/PEDOT/GNP/GDL electrode indicates that an increase in the activity for CO electro-oxidation is achieved by replacing Pt with PtW. This may be attributed to structural changes caused by alloying and the increased conductivity and high specific surface area of PEDOT and GNPs catalyst support, respectively. CV scanning results showed that the PtW/PEDOT/GNP/GDL electrode has greater stability than the Pt/C/GDL electrode

1. Introduction

Proton exchange membrane fuel cells (PEMFCs) have drawn a great deal of attention as energy conversion devices in recent years due to their high efficiency and low/zero emissions. Direct methanol fuel cells (DMFC) have been attracting huge research interest as power sources for vehicles and portable

*Corresponding Author's Fax: +984432775660
E-mail address: m.yaldagard@urmia.ac.ir

doi: 10.22104/ijhfc.2019.3549.1187

electronic devices [1-4]. However, to become commercially viable, PEMFCs have to overcome the barrier of high catalyst cost caused by the exclusive use of platinum and platinum-based electrocatalysts [5, 6] in both oxidation of fuel and reduction of oxygen at the fuel-cell electrodes. Recently, many researches about fuel cells have been dedicated to the electrode material, including various forms of carbon, transition metal oxides, and conducting polymers, relating to the development of bimetallic/ alloy Pt–based electrocatalysts [7-14]. Among the Pt alloys, the PtRu system has been the most extensively investigated for DMFC applications. However, there is increasing interest in the exploration of other Pt alloy systems involving metals such as Ni, Fe, Sn, Mo, Os and W [15-20]. Recently high throughput combinatorial studies have demonstrated that PtW alloy films present superior catalytic activities in methanol oxidation [21-23]. Based on these literature findings, we deem it meaningful to explore the carbon supported PtW catalysts effective for DMFC applications. In comparison with other Pt bimetalic electrocatalyst samples, PtW offers several benefits: (i) the amount of Pt can be reduced dramatically due to the low Pt content (~35 wt%) in a PtW (1:2) bimetallic catalyst, whereas other PtM bimetallic electrocatalyst (with a Pt:M of 3:1, where M = Co, Ni, etc.) have Pt contents of more than 90 wt%; (ii) a PtW electrocatalyst will not damage a fuel cell even if it diffuses to the anode due to dissolution; in another words, W has high tolerances towards anode catalyst poisons [24]; and (iii) a recent study showed that W itself is utilized as a catalyst for H2O2 decomposition, thus PtW effectively inhibits nafion membrane damage due to H_2O_2 formation [25].

Furthermore, the catalytic performance of DMFC depends on the nature of its support material and preparation techniques. Conducting polymers (CPs) have received much attention owing to their high surface area, high electrical conductivity, and high stability [26]. Electrically conducting polymers have also been intensively investigated as electrode materials because of their electrochemical reversibilities, fast switching, high conductivity, mechanical flexibility, low toxicity, and low cost [27-29]. Given their conductive and stable three dimensional construction, CPs can act as appropriate supports for low temperature fuel cell catalysts. Unlike carbon and ceramic materials where the catalyst is localized on the support surface (2D), in conductive polymer support the catalyst can be also dispersed inside the matrix (3D) depending on the deposition method, catalyst loading, and polymer thickness [30]. Conducting polymer/ metal–nanoparticle composites allow a facile flow of electronic charges through the polymer chain during the electrochemical process. Moreover, CPs provide a low ohmic drop for the electron transfer between the metallic catalyst and the supports. CPs with porous constructions and high surface areas are employed as a matrix to integrate metallic catalysts for some vital electrochemical reactions used for application in fuel cells such as methanol oxidation [30]. Among conducting polymers, poly 3,4-ethylenedioxythiophene (PEDOT) can be used as the active electrode material due to its remarkably high conducting and unusual environmental stability in PEMFC condition [31]. Composites of PEDOT and several kinds of carbon nanomaterials, i.e, CNTs and graphene, are usually prepared to improve electrochemical performance [32-35]. Lota et al. reported the capacitance properties of PEDOT/ CNT composite material in 2004 [36]. Chen et al. synthesized core-shell PEDOT/poly (sodium 4-styrenesulfonate) / CNT as an electrochemical supercapacitor [37]. Chu et al. [38] synthesized PEDOT-modified graphene composite materials as flexible electrodes for energy storage and conversion applications. Hence, PEDOT is viewed as a suitable candidate for energy storage applications on nanocarbon surfaces.

Graphene, a one-atom thick layer of sp^2 carbon atoms firmly packed into a honeycomb lattice, have potential application as a catalyst support in DMFCs owing to its high surface areas, supreme electric conductivities, and distinguished mechanical properties. As described in our previous paper [39], the acute problems associated with the investigation

of graphene sheets as catalyst support in chemical method, specifically irreversible agglomerates of reduced graphene sheets because of Vander Walls interaction and even recumulate to form graphite in the reduction from graphene oxide suspension or drying procedures, have been resolved using an electrochemical reduction system. Moreover, it is vital for the Pt particles to be located in the three-phase reaction zones. In the conventional chemical method the inactive sites are not in good contact with the electrolyte phase; consequently, the catalyst is not fully utilized. Electrodeposition as a green in-situ method offers a unique way to deposit many metals, selectively, at desired sites in the substrate through simply controlling the nucleation and growth of the metal nanoparticles. Using this method insures that the catalyst ions in the plating bath would pass through the electrolyte to the support materials and be deposited on those regions where protonic and electronic conduction coincided. More information about the electrochemical method as a green in-situ method in reducing the graphene oxide to graphene nanoplates and electrodeposition of catalyst on substrate can be find in our previous work [39].

In this study, 3 principle approaches have been explored to reduce the cost of fuel cell catalysts: (i) increase Pt catalytic activity and reduce Pt content through alloying with other transition metals such as W, (ii) Enhancement of electrocatalytic efficiency by using high electrically conductivity and more stable support, and (iii) Improve Pt utilization by both increasing the surface area/dispersion of Pt nanoparticles using high-surface area support and using the galvanostatic electrodeposition method. These approaches effectively create electrocatalysts with robust activity towards the methanol oxidation reaction. Accordingly, this study focuses on the electrodeposition of bimetallic PtW on reduced graphene nanoplates (GNPs) on the gas diffusion layer (GDL, carbon paper) in PEDOT electropolymerized in constant voltage, here after known as the PtW/PEDOT/GNP/GDL electrode. Compared to our previous study [39], this new research proposes a design to enable synergistic effects in GNP, PEDOT, and PtW by using PtW as a more effective electrocatalyst for DMFC application. PtW is more effective due to its high tolerances towards anode catalyst poisons, while PEDOT is a conductive polymer which may favor adhesion onto the graphene surface and is highly conductive which is beneficial for electronic and ionic transport.

2. Experimental

2.1 Materials

Most of the material used in this work are similar to our previous work [39] except for Tungsten chloride (99.999%), 3, 4(ethylene dioxy thyophene, 97%), sodium dodecyl sulfate (SDS) which were all obtained from Sigma Aldrich, and CO (99.99%) gas which was purchased from Canadian Sigma Inc.

2.2 Methods

2.2.1 Electro- polymerization of EDOT on GNP

An electrolyte of 0.1M H_2SO_4 +0.01M EDOT +0.01M SDS was used for PEDOT deposition. The electrodeposition was carried out potentiostatically at 0.9V as reported by Patra et al. [40]. The solubility problem of the monomer (EDOT) in water was resolved by adding chosen surfactants, which can be anionic, such as sodium dodecyl sulfate (SDS) [41, 42]. Also as reported in the literature, the SDS exhibited an electrocatalytic effect, characterized by a decrease of the EDOT oxidation potential (the oxidation potential of thiophene (1.8 V) is higher than that of water (1.23V) [43], which may result from strong electrostatic interactions between the EDOT cation radical and SDS anions [41]. Fig. 1 shows the quantity of PEDOT deposited on the substrate.

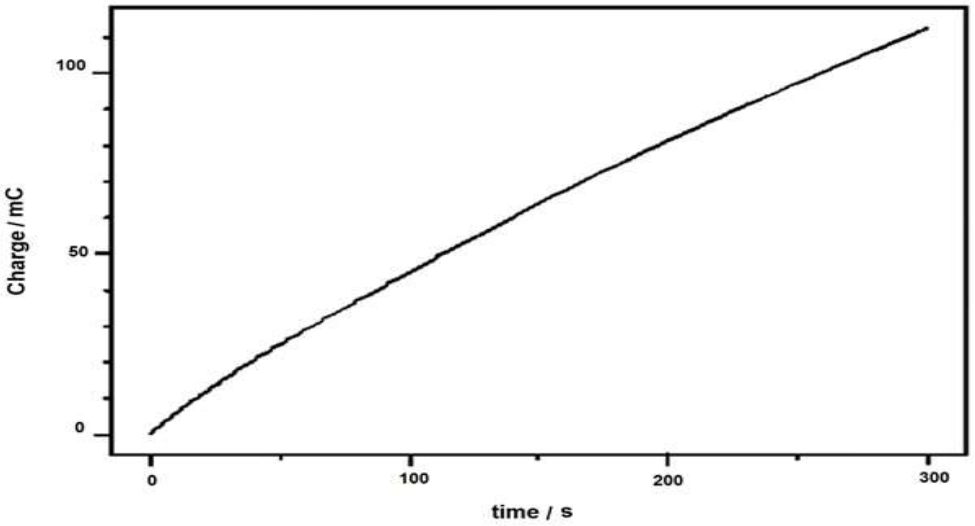

Fig. 1. The quantity of PEDOT deposited on the substrate

2.2.2 Synthesis of PtW Nanoparticles on PEDOT/GNP based Carbon Paper

The procedure of the synthesis of PtW nanoparticles on PEDOT/GNP based carbon paper are the same as our previous work [39] with only slight changes as explained below:

The PEDOT/GNP on GDL served as a cathode and the Pt foil as an anode electrode. Electrodeposition was performed in a plating bath containing a solution of 4mM $H_2Pt\ Cl_6.6H_2O$ + 10mM WCl_4 dissolved in 0.5 M NaCl. The concentration values of 4mM for $H_2PtCL_6.6H_2O$ and 10mM WCl_4 were selected because in these concentration the optimum atomic ratio of 1:1 PtW were found to provide the highest performance (not bring here). Total amount of charge was 1,200mCcm^{-2} (Fig. 2).

It must be mentioned that the chemical preparation of graphene oxide (GO), electrode preparation, and in situ electrochemical reduction of graphene nanoplates (GNP) were conducted in the same manner as our previous published work and the details are reported in [39]. In brief this study involved three chemical electrochemical procedures. Exfoliated graphene oxide was first prepared by using the modified method of Hummers and Offeman [44, 45]. The nanocomposite film of PtW nanoparticles deposited on the electropolymerized PEDOT on the exfoliated graphene sheet/carbon paper was then obtained using a two successive electrochemical reduction and deposition routes.

2.3 Characterization

All of the equipment used to analyze the characteristics of the samples are the same as reported in our previous work [39]. Additional items are as follows: The electrical conductivity of the film samples was measured on a ZCLT3A using a four point configuration. The electrochemical reduction of graphene, electropolymerization of EDOT, and PtW electrodeposition as well as cyclic voltammetry measurements, methanol oxidation and CO stripping experiments were carried out using a potensiostat/ galvanostat model Iviumstat XRi electrochemical Interface System.

3. Results and discussion

3.1 Fabrication of Electrochemically Reduced Graphene Nanoplates (GNP) on a Carbon based Electrode

The resultsof the fabrication of electrochemically reduced GNP on a carbon based electrode have been discussed in a prior paper [39]. Only the number of CV scans in the electrochemical reduction of GO

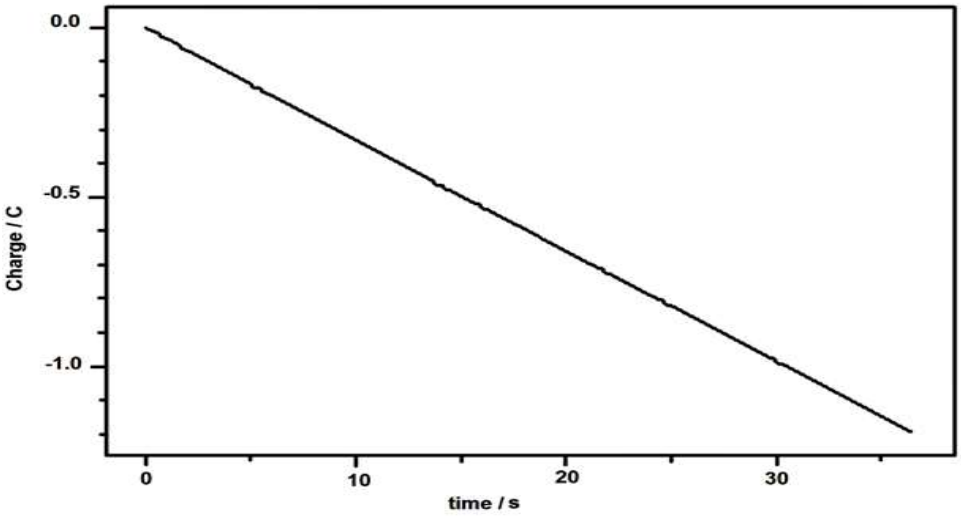

Fig. 2. The quantity of PtW deposited on the substrate

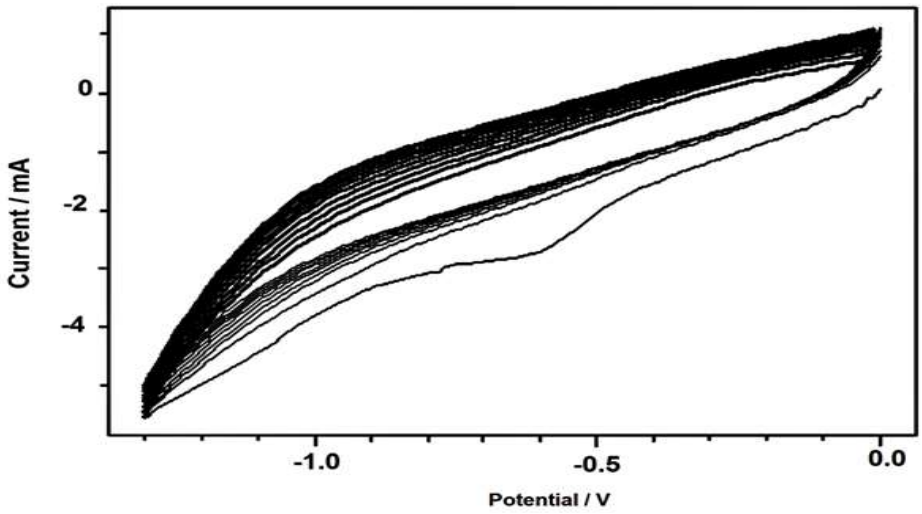

Fig. 3. Cyclic voltammetry curves of GNP film on carbon paper electrode in the aqueous solution of 0.1M KCl at a scan rate of 10 mVs^{-1} for 10 segments

in the former was 5, while the present work was conducted in 10 segments (Fig. 3).

3.2 Deposition profile of PEDOT on electrode surface

The electrochemical procedures used for EDOT polymerization were fixed potentials of 0.9V vs. SCE during 300s. The deposition of PEDOT polymer at the electrode surface is indicated by the increase in the charge from 0 to 110mC for 300s (Fig 4.) This condition is expected to ensure the polymerization of the monomer but avoid the degradative cross-linking reactions that typically take place at higher potentials. Uniform, adherent, insoluble, and dark-blue polymer films grew on the surface of the electrode. Fig. 4 shows the resulting chronoamperogram obtained for the oxidation of a 1mM EDOT aqueous solution with 10Mm SDS. The electrodeposition curve of PEDOT from a monomer solution at a constant potential of 0.9V for 300s shows a trend characteristic of thiophene oxidation [46]. As soon as the potential is applied the current rises spontaneously and a peak is observed at 0.45 mA due to the double-layer capacitance charge, which is immediately followed by an exponential decay. The current density stabilizes at 0.15$mAcm^2$

for PEDOT electropolymerization in the presence of SDS. In fact, a plateau corresponds to polymerization and the smooth deposition of the PEDOT film on the electrode surface for the subsequent duration of deposition. A similar trend for current–time transient was observed by others [47] for EDOT-oxidation and electropolymerization in a protonic organic electrolyte. The CV curves of the PEDOT/GNP/GDL and GNP/GDL electrode in 0.1M KCl solution with a scanning rate of 50mVcm^{-1} are displayed in Fig. 5. The electrodes were cycled between0.24V and 1.2V. Generally, the rectangular shape of CV curves (no oxidative or reductive peak) explains the typical behavior of the electrical double layer (EDL) capacitive behavior [48]. As can be seen in Fig. 5, the curves of the electrodes in the current study exhibit oblique and narrow CV loops. This behavior is attributed to the poor electrolyte/electrode interfacial contact [49, 50]. However, the closed CV loop of the GNP/GDL is very small signifying low capacitance value due to the deficient of electroactive sites on the surface. Whereas, the PEDOT/GNP/GDL illustrates a larger closed CV loop compared with GNP/GDL revealing higher EDL capacitance values. The explanation agreed with the calculated capacitance value of the polymers from the CV measurement.

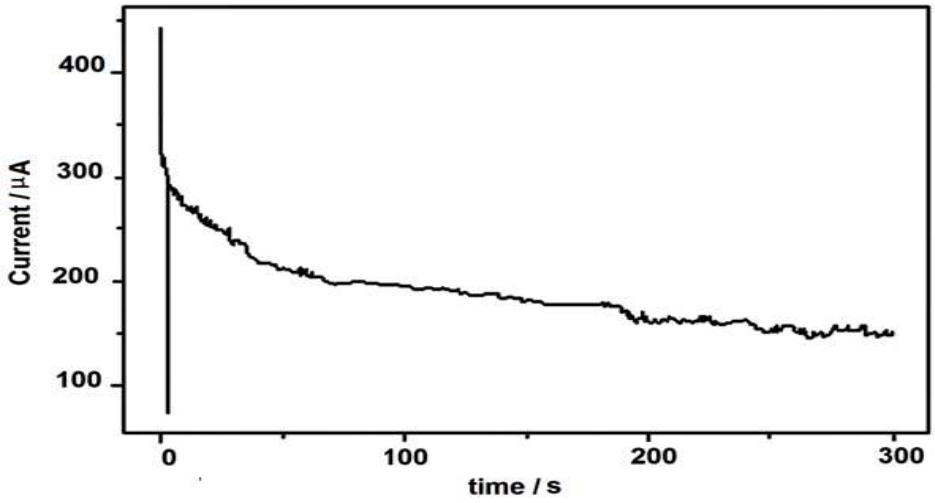

Fig. 4. Chronoamperograms recorded for oxidation of a 0.01 M 3,4-ethylendioxythiophene solution in 0.1M H_2SO_4 +0.01 M SDS on PEDOT/GNP/GDL electrode by applying a constant potential 0f 0.9V for a polymerization time of 300s

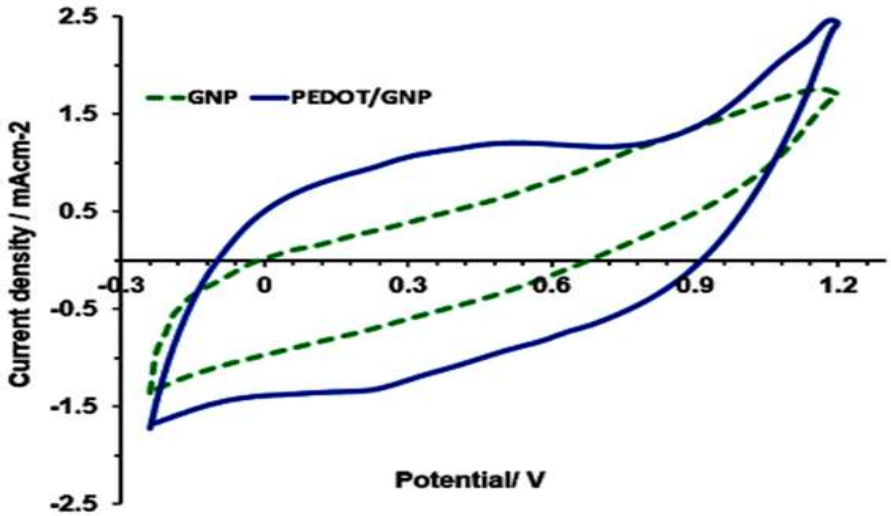

Fig. 5. The CV curves of PEDOT/GNP/GDL and GNP/GDL electrode in 0.1M KCl solution with a scanning rate of 50mVs^{-1}

3.3 Topography of electrodes

Figure 6 shows an AFM image of PEDOT polymerized on graphene nanoplates along with corresponding height profile. As seen from the Fig. 6, PEDOT closely covers the surface and the edges of the GNP layers during the in situ electropolymerization of 3,4-ethylenedioxythiophene. Explanation about the AFM image of the GDL surfaces with and without graphene nanoplates produced by electrochemical reduction from dispersed graphene oxide were given in [39].

3.4 Morphology and Structural Characterization of Prepared Electrode

Fig. 7 shows the FT-IR spectra of PEDOT electropolymerizied on GNPs. In the PEDOT/GNP/GDL electrode the successful formation of PEDOT on GNP is evidenced by the presence of peaks at 1513, 1540, 1556 ,1650 and 1330cm^{-1} (C = C and C- C stretching vibrations of the thiophene ring), 1064 and 1089cm^{-1} (C- O- C bond stretching), and 981, 844, and 667cm^{-1} (C -S bond in the thiophene ring) [51]. The peak at 1513cm-1, which is related to the asymmetric C = C stretching vibration of the quinoidal structure originating from the thiophene ring, was clearly observed. Additionally, the stretching of C=C in the thiophene ring is related to the peak around 1461cm^{-1} to 1833cm-1 [52-55]. The peak at 1330cm^{-1} in the literature [56] is the C-C stretching mode, which shifted to 1336cm^{-1}. The peaks at 1207 and 1137 cm^{-1} are attributed to the vibration modes of the ethylenedioxy group in the molecule of PEDOT [57].

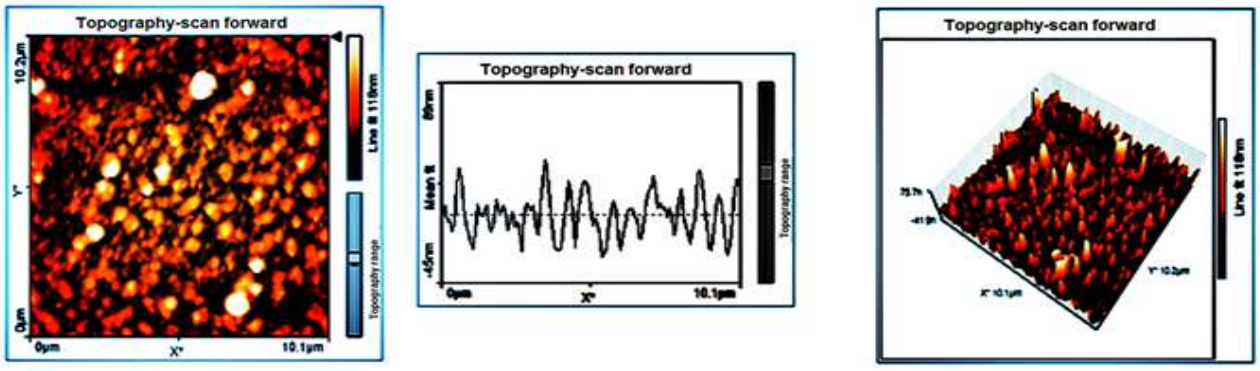

Fig. 6. AFM topography images of electropolymerizied PEDOT on GNP

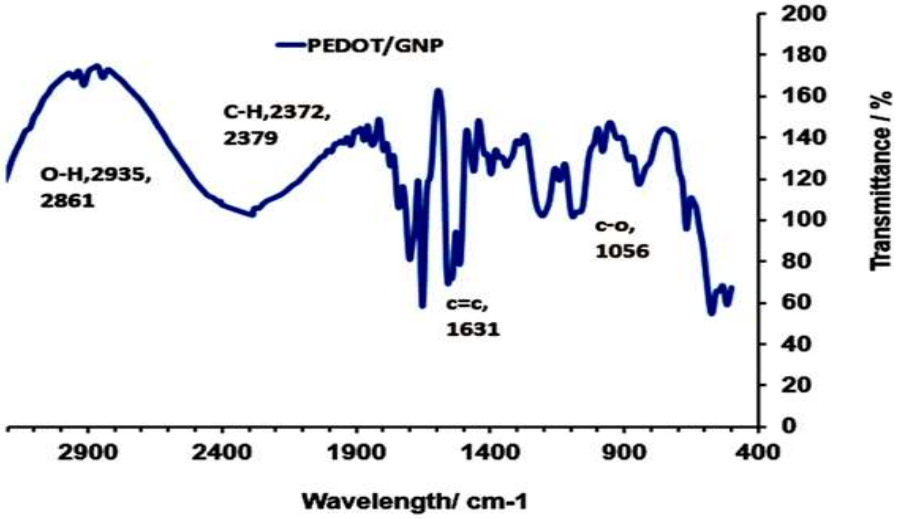

Fig. 7. FT-IR spectra of PEDOT on in situ reduced graphene nanoplates harvested from the carbon paper substrate

The C-O-C deformation modes, which are reported at 1060 and 1086 cm^{-1} in the literature, shifted to 1064 and 1089cm^{-1}, respectively. C-S bonds in the thiophene ring are seen in 667, 844, and 981cm^{-1}. The oxyethylene ring deformation stretching mode, which was reported at 840cm^{-1} in the literature, was seen at 844cm^{-1}. Finally, the symmetric C-S-C deformation, which was reported at 691cm^{-1} in the literature, appeared in 667cm^{-1} [56]. Thus, the discrepancies in above-mentioned peaks suggested that the PEDOT was successfully grown on the substrate. The FTIR spectra of the pristine graphite, graphene oxide (GO), and electrochemical reduced GNPs were to a great extent reported in our previous work [39].

Fig. 8 shows the typical Raman spectra of PEDOT polymerized on GNP/GDL. The Raman spectrum of the PEDOT/GNP/GDL electrode reveals the main peaks of PEDOT to be 1436cm^{-1} (C=C symmetric stretching) and 1512cm^{-1} (C=C asymmetric stretching). The G and 2D peaks were observed at 1588 and 2614cm^{-1}, respectively. However, the characteristic peaks of PEDOT in the region of D and G peaks make it difficult to confirm these peaks in the hybrid electrode. The Raman bands, which show the fundamental vibrations modes of PEDOT, were located at 1364, 1432 and 1512cm^{-1}. They are assigned to the single C-C stretching, C=C symmetric stretching, and C=C asymmetric stretching, respectively [58, 59]. The Raman spectrum of GO and GNP were also reported in [39]. Fig. 9 shows the X-ray diffraction patterns of the PtW/PEDOT/GNP/GDL and Pt/C/GDL electrodes, which reveal the diffraction peaks of both carbon and platinum. The sharper and narrow diffraction peaks at $2\theta=26.53^{o}$(002) and 54.507^{o}(004) are characteristics of the parallel graphene layers in the PtW/PEDOT/GNP/GDL electrode, which indicate the highly graphitic and crystallinity ordered structure of GNP in planes of (002) and (004), respectively, while a strong peak at about $2\theta=26.45^{o}$ in the Pt/C/GDL electrode could be attributed to XC-72 carbon present in commercial Pt/C of the fuel cell earth.

High resolution XRD spectra obtained over the range $2\theta=35\text{-}90^{o}$ from the electrodes are given in Fig 9.b. The peaks at the Bragg angles of 41.46^{o}, 45.48^{o}, 69.28^{o}, and 86.77^{o} corresponds to the (111), (200), (220) and (222) crystalline plane diffraction peaks, respectively. All peaks can be indexed as the Pt face centered cubic (fcc) phase. The formation of PtW alloy in the PtW/PEDOT/GNP/GDL electrode was confirmed by a slight shift of XRD patterns to higher angles due to the contraction of lattice relative to the Pt/C/GDL electrode, signifying that the interatomic distance of platinum has been diminished by replacement of the smaller W atom into the Pt lattice (Table1). Furthermore, there were no well-defined diffraction peaks conforming to the presence of any metallic W or oxide phases. This is possibly because the W loading was relatively low and any metal

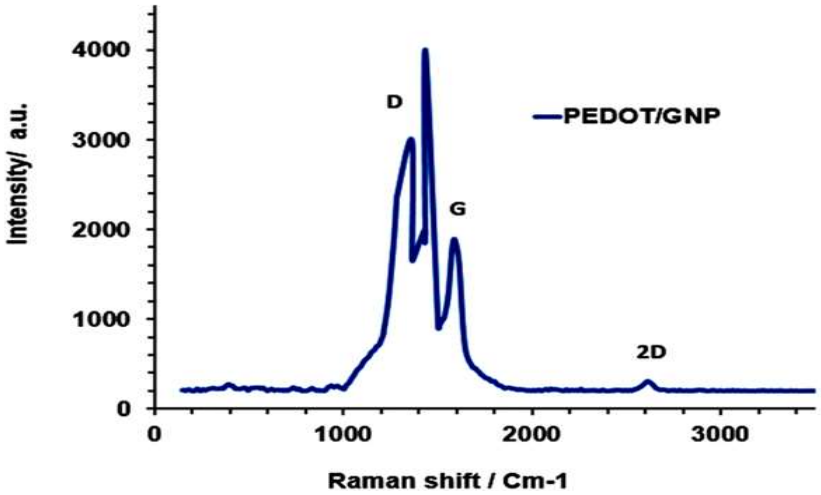

Fig. 8. Raman spectrum of PEDOT on GNP

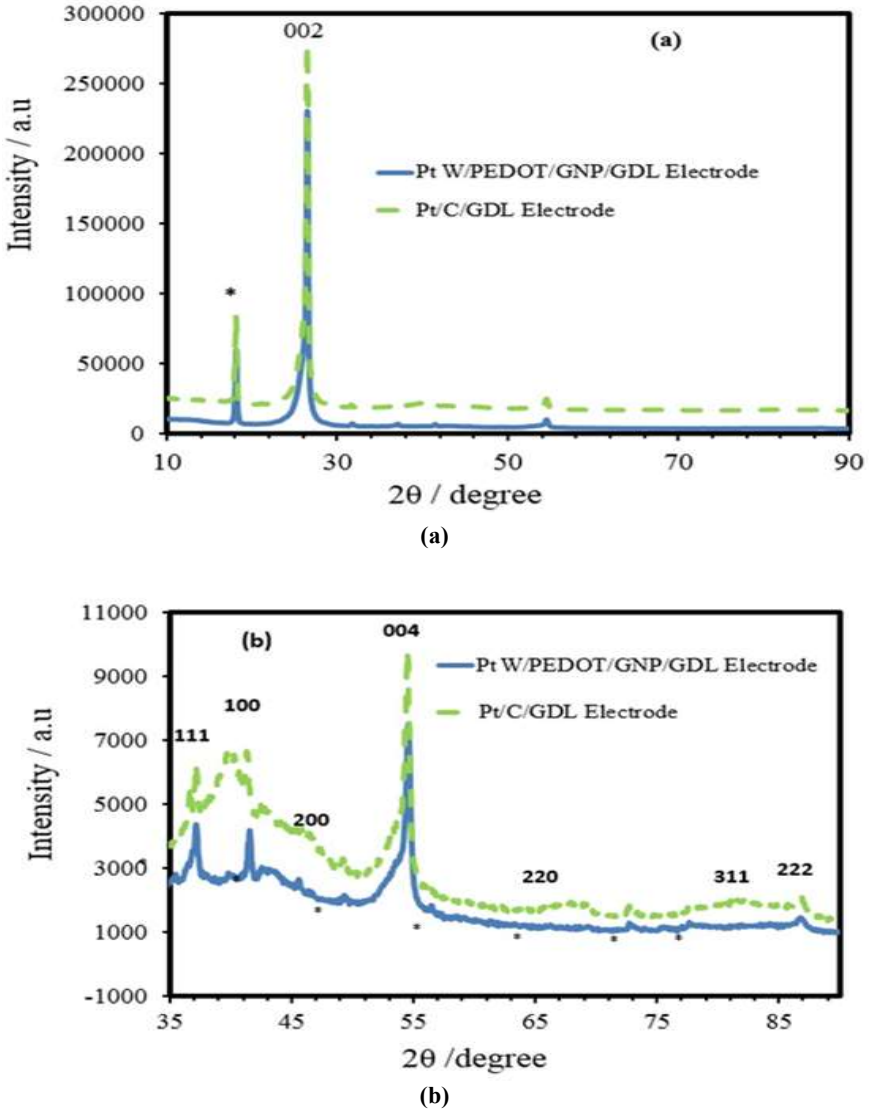

Fig. 9. X-ray diffractograms of the a)PtW/GNP/GDL and Pt/C/GDL electrodes, b) High resolution XRD spectra obtained over the range 2θ=35-90 from the electrodes

Table 1. Chemical composition and structural parameters of Pt/C/GDL and PtW/PEDOT/GNP/GDL electrodes, EDS composition, lattice parameters (nm), W atomic fraction in the alloy(x), and crystal size.

Electrode	EDS composition (Pt/W)	Lattice parameter/nm	x	degree of alloying	2θ	crystallite size (XRD)/nm	d-spacing/nm
Pt/C/GDL	-	0.3907	0	-	39.4	4.20	0.2256
PtW/PEDOT/GNP/GDL	59:41	0.3690	0.131	0.28	41.46	18.57	0.2176

W species present were greatly dispersed or were amorphous and therefore could not be identified. The peaks of the as prepared PtW/PEDOT/GNP/GDL electrode are sharper than those of the Pt/C/GDL electrode, demonstrating that they have larger particle sizes than the commercial supported platinum. The average size of Pt particles were considered from the Debby-Scherrer equation using the full width at half maximum (fwhm) of the (111) reflection. Pt (111) plane was chosen for Scherrer analysis because it has the highest intensity value.

Considering that Vegard's law applies to the

PtW/PEDOT/GNP/GDL electrode, the degree of alloying and W atomic fraction in the PtW alloy (x) according to the variation of lattice parameter on cobalt content was calculated from the expressions below:

$$X_a = \frac{a - a_0}{a_c - a_0} \quad (1)$$

$$x = X_a \times x_c \quad (2)$$

Where a_0 and a_c are the lattice parameter of supported platinum (0.3907nm) and the lattice parameter assuming that all the tungsten is alloyed (0.3164nm), respectively [60]. a is the experimental lattice parameter of PtW (0.3690nm), and xc is the W atomic fraction (0.47) in the PtW catalyst. The values of Xa and W atomic fraction in the alloy (x) are presented in Table 1.

Fig. 10 shows the surface morphology of the in situ reduced graphene nanoplates on carbon paper, the PtW electrodeposited on PEDOT coved in situ reduced graphene nanoplates on carbon paper, and the Pt/C nanoparticles sprayed on the carbon paper. Fig. 10(a) shows the SEM image of GNP, which displays an ensemble of two-dimensional micrometer-sized graphene plates with obvious spacing among the plates. A relatively high density of in situ reduced graphene nanoplates over all the surface of the fibers of the carbon paper substrate is seen from Fig. 10(a). Fig. 10(b) shows the FSEM after the electrodeposition of PEDOT on the GNP/GDL and illustrates that many white particulates have grown on the wrinkled sheets of the graphene. Sponge and porous morphology can be observed in Fig. 10(c) after coating PEDOT on the graphene plates on GDL to form the PEDOT/GNP/GDL.These aggregates of PEDOT densely cover the surface and the edges of the GNP layers, implying the existence of a strong

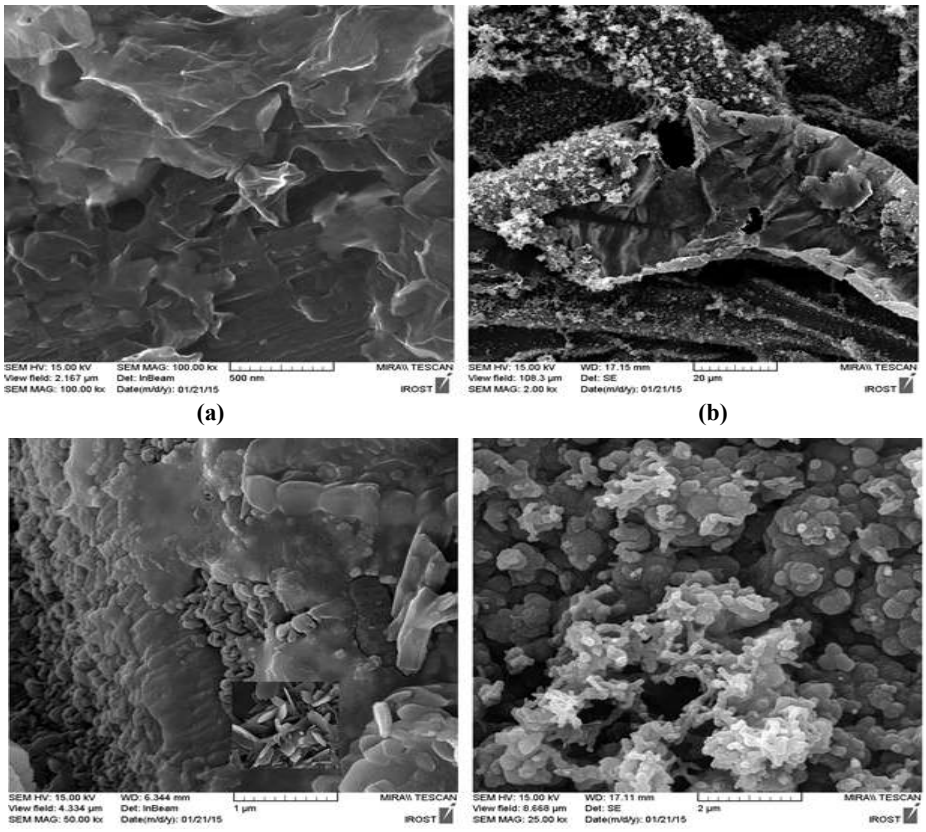

Fig. 10. FE-SEM images of the a) in situ reduced graphene nanoplates on carbon paper b,c) electropolymerized PEDOT on GNP d)PtW electrodeposited on PEDOT/GNP/GDL

interaction between PEDOT and GNP. The high-magnification FSEM image in the inset of Fig.10(c) reveals the sheet-like spongy structure of PEDOT, which is approximately several hundred nanometers in particle size. Fig. 10(d) shows the SEM image after the electrodeposition of PtW catalyst on PEDOT/GNP/GDL, and there are spherical PtW particles on the PEDOT/GNP/GDL with a higher density. Fig. 11 compares the SEM images of PtW/PEDOT/GNP/GDL and Pt/C deposition on GDL.

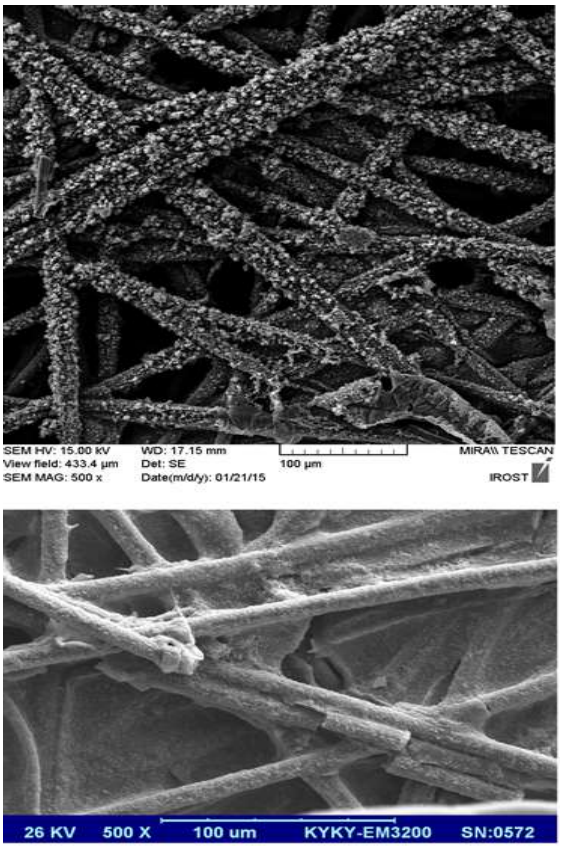

Fig. 11. SEM images of the (up) PtW/PEDOT/GNP/GDL (down) Pt/C nanoparticles on fibers of carbon paper

Further characterization on the PEDOT synthesized on the GNP in the electrochemical cell, complementary to FTIR measurements, was carried out using EDS. Fig. 12 shows the typical EDS pattern of the PtW/PEDOT/GNP/GDL electrode. It shows that the prepared electrode contains both of Pt and W elements. The EDS pattern shows that C, O and F are the major portion of spectra. The C signal comes from the graphene nanoplates and Nafion solution. Oxygen, S and F are also derived from Nafion. A small segment of oxygen may be resulting from the incomplete reduction from graphenen oxide to graphene. In addition to Pt, W, O, C and F, the element of Si and K were noticed as well. The strong peak of Si is due to the silicon substrate used in FESEM analysis. The relatively trivial amount of K observed in the EDS image is basically from the KCl electrolyte used in the plating bath. The existence of a sulfur element for PEDOT/GNP/GDL confirms again the successful polymerization of EDOT.

3.5 Electrical conductivity of the nanocomposite

The electrical conductivity of the film samples of GNP/GDL and PEDOT/GNP/GDL was measured on ZCLT3A using a four point configuration method according to ASTM Standards F43-93 at room temperature. The results showed considerable conductivity for 3, 4 ethylen dioxy thiophene on nanoplates of graphene on a gas diffusion electrode with the value of 56 S/cm with respect to the nanplates of graphene on a gas diffusion electrode with the value of 43 S/cm.

3.6 Electrochemical analysis

Fig. 13 shows typical steady–state cyclic voltammograms of Pt/C/GDL and PtW/PEDOT/GNP/GDL electrodes prepared using galvanostatic pulse electrodeposition. For cyclic voltammetry (CV) measurements, the working electrode was immersed in 0.5 M H_2SO_4 solution saturated by high purity (99.9995%) nitrogen with the potential range between -0.24 and 1.2V vs Ag/AgCl (saturated KCl). The scan rate was set at 50mVs^{-1}. Before the experiment a Nafion solution was impregnated to develop the three-dimensional reaction zones in the electrode. All given potentials were converted and reported in the reversible hydrogen electrode (RHE) scale.

The electrochemical Pt surface areas of catalysts (S_{ESA}), the real specific area, S_{CSA}(m^2g^{-1}) (one of the most important parameters characterizing the surface

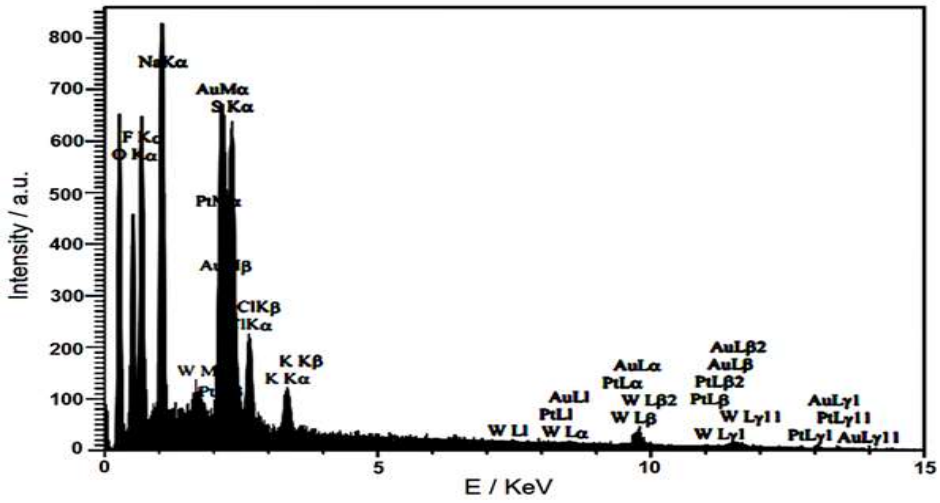

Fig. 12. EDX pattern of PtW deposited on PEDOT/GNP/GDL

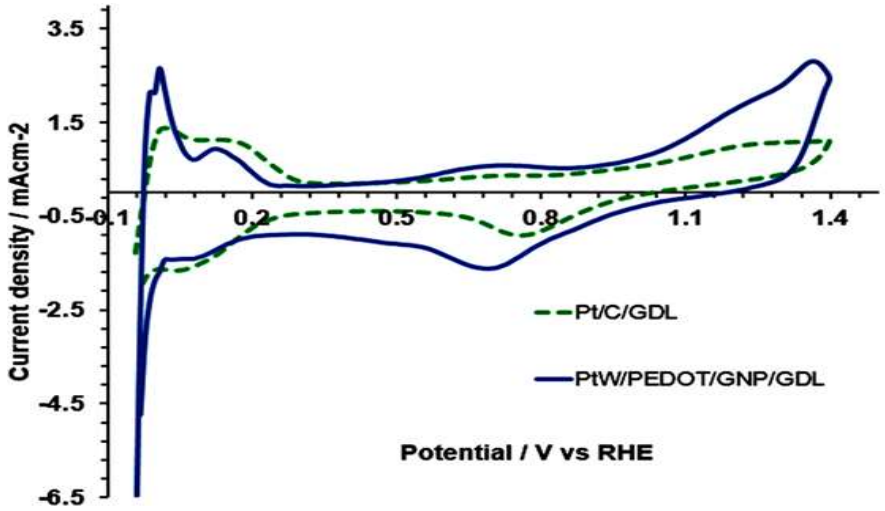

Fig. 13. Cyclic voltamograms of PtW/PEDOT/GNP/GDL and Pt/C/GDL in 0.5M H_2SO_4 solution scan rate: 50 mVs^{-1}

Table2. Electrochemical surface area of Pt/C/GDL and PtW/PEDOT/GNP/GDL electrodes in N_2 saturated solution of 0.5M H_2SO_4

Electrode	Pt loading /$mgcm^{-2}$	SESA/$m^2Ptmg^{-1}Pt$	SCSA/ $m^2Ptmg^{-1}Pt$	γ_{Pt} (%)
Pt/C/GDL	1	35.37	66.75	53
PtW/PEDOT/GNP/GDL	0.57	14.48	15.09	96

of solid electrodes for the crystallites), and the Pt utilization efficiency were determined by equations presented in a former work [39]. Table 2 presents the corresponding calculated values of SESA, SCSA and γ_{Pt}.

It must be mentioned that the real chemical surface area is different from the geometric area. In contrast to liquid electrodes (i.e. mercury), the surface of a solid electrode is always not smooth and its real area exceeds the geometric one [61]. In the case of electrocatalytic materials the S_{CSA} may even be 1000 times greater that the geometric area [62] and this differs for different electrodes.

The real chemical surface area (S_{CSA}) of the prepared electrocatalyst can be calculated using Eq. 3:

$$S_{CSA} = \frac{6\times10^3}{\rho d} \quad (3)$$

Where ρ is the density of Pt (21.4 gcm^{-2}) and d is the mean diameter of the Pt nanoparticles obtained from

XRD (in nm).

The compression of cyclic voltammograms of Pt/C/GDL and PtW/PEDOT/GNP/GDL electrodes in Fig.13 shows that tthe double-layer thickness of the PtW/PEDOT/GNP/GDL electrode is somewhat inferior than the Pt/C/GDL electrode due to the addition of W. Moreover, the current density of the hydrogen release region increases with the addition of W, revealing the change in electrochemical active surface area with the addition of W within the catalyst. The electrochemical surface areas (ESA) of Pt/C/GDL and PtW/PEDOT/GNP/GDL electrodes are tabulated in Table 2. It can be seen that the bimetallic PtW/PEDOT/GNP/GDL electrode had a lower Pt surface area (15.09 $m^2.mgPt^{-1}$) than the monometallic Pt/C/GDL electrode (66.75 $m^2.mgPt^{-1}$). This was predictable because some Pt surface atoms are covered by W atoms. However, the PtW/PEDOT/GNP/GDL electrode depicts greater utilization than the Pt/C/GDL electrode. This behavior has been reported by others in Pt-Co [63], Pt-Pd systems [13], etc. It is clear that nanoparticles in the PtW/PEDOT/GNP/GDL electrode were deposited favorably on electrochemically more active sites, i.e, PEDOT covered graphene edges and torsions, giving escalation to a strong interaction with the substrate and a deterministic increase of utilization efficiency. To the best of our knowledge, such utilization, (96%) for the PtW alloy considering the mean particle size, is outstanding when compared to the published results. The smaller electrochemical surface area value of the PtW/PEDOT/GNP/GDL electrode in comparison to the Pt/C/GDL electrode can also be explained by XRD results. The reduced Pt surface area of the PtW/PEDOT/GNP/GDL electrode is consistent with its higher particle size produced by alloying.

3.7. Performance Evaluation of Catalyst through the Methanol Oxidation Reaction (MOR) and CO Tolerance

Fig. 14 displays the cyclic voltammograms for the PtW/PEDOT/GNP/GDL and commercial Pt/C/GDL recorded in 0.5M H_2SO_4+1M CH_3OH at a scan rate of 50mVs^{-1}. As can be seen, the first methanol electro-oxidation peak potential in the forward scan is located at around 0.69V for PtW/PEDOT/GNP/GDL, which is slightly lower than that of the Pt/C/GDL (0.71V), suggesting higher activity for methanol oxidation on the PtW/PEDOT/GNP/GDL electrode. Also, the PtW/PEDOT/GNP/GDL catalyst displays a particularly higher current density of 4.45 $mAmgPt^{-1}$ at a lower onset of 0.21V potential compared with that of 3.61 mA $mgPt^{-1}$ and 0.43V for the Pt/C/GDL electrode, demonstrating that PtW/PEDOT/GNP/GDL exhibits a higher catalytic activity for methanol electro-oxidation than Pt/C/GDL. In addition, the observation of much higher If/Ib values on PtW/PEDOT/GNP/GDL (1.82 vs 1.78 on Pt/C/GDL) signifies that methanol molecules are more effectively oxidized on PtW/PEDOT/GNP/GDL during the forward potential scan, generating much less poisoning species compared with commercial Pt/C/GDL. This could be due to the mixed-conducting nature of PEDOT which enhances proton and electron transport within the anode catalyst or the synergistic effects between Pt nanoparticles and the PEDOT/GNP support [64, 65]. From the above obtained results, it is concluded that the PtW/PEDOT/GNP/GDL electrode showed a superior performance for methanol electro-oxidation than that of Pt/C/GDL.

Further examination was made into transport behavior of methanol on the nanocomposite electrocatalyst. From Fig. 15, it can be seen that the peak current density of methanol oxidation increases with the increase of scan rates and the peak potential has almost no significant change. The inset in Fig. 15 indicates that the anodic peak current densities are linearly proportional to the square root of the scan rate, which reveals that the electrocatalytic oxidation of methanol on the nanocomposite electrocatalyst is a diffusion-controlled process [66].

As CO species are the main poisoning intermediates during the methanol electro-oxidation, a fine electrocatalyst for methanol oxidation should possess exceptional CO electro-oxidation ability and high tolerance, which can be evaluated by CO stripping

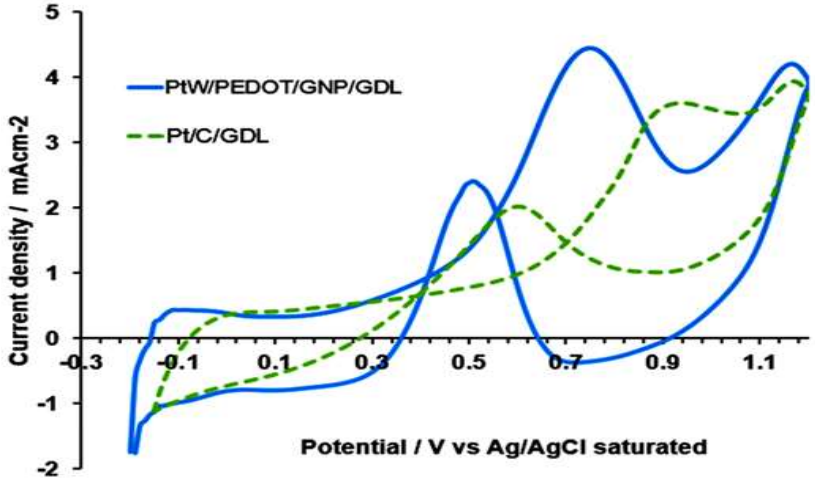

Fig. 14. Cyclic voltamograms of methanol oxidation of PtW/PEDOT/GNP/GDL and Pt/C/GDL in 0.5M H_2SO_4 +1M CH_3OH solution scan rate: 50 mVs^{-1}

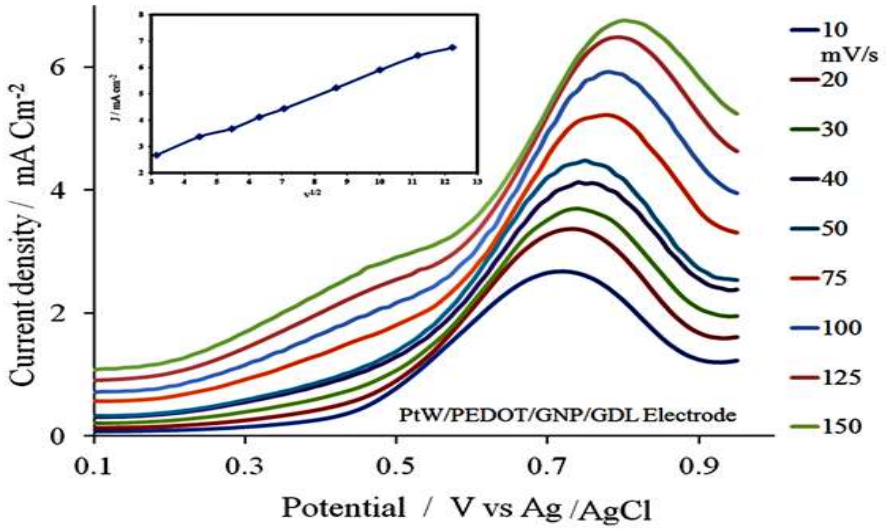

Fig. 15. The anodic peak current densities of PtW/PEDOT/GNP/GDL in 0.5M H_2SO_4 +1M CH_3OH solution at different scan rates. The inset shows the dependence of the anodic peak current densities on the square root of scan rates.

voltammetry. Fig 16 shows the CO stripping voltammograms on PtW/PEDOT/GNP/GDL and Pt/C/GDL, which was performed by electro-oxidation of pre-adsorbed CO. The peak at about 0.75V and 0.92V vs Ag/AgCl represents the electro-oxidation of the irreversibly adsorbed CO on PtW/PEDOT/GNP/GDL and Pt/C/GDL, respectively. The intended peak charge, Q_{CO}, is related to the reaction:

$$Pt - CO + H_2O \rightarrow Pt + CO_2 + 2e^- + 2H^+ \quad (4)$$

the charge Q_{CO} ($mCcm^{-2}$) was used to compare the active surface area of the catalyst ESACO, from the equation reported in [67].

The ESA values calculated from the CO electro-oxidation area, ESA-CO are 11.09 and 5.63 m^2g^{-1}. for the PtW/PEDOT/GNP/GDL catalyst and Pt/C/GDL, respectively. The higher ESA-CO of the PtW/PEDOT/GNP/GDL catalyst indicates higher Pt utilization in the PtW/PEDOT/GNP/GDL electrode. Therefore, the PtW/PEDOT/GNP/GDL electrode could contribute to enhanced activity toward CO oxidation. Also, the electro-oxidation current of the CO_{ads} species on the PtW/PEDOT/GNP/GDL is around 1.78 $mAcm^{-2}$, which is higher than that of Pt/C/GDL, indicating that the PtW/PEDOT/GNP/

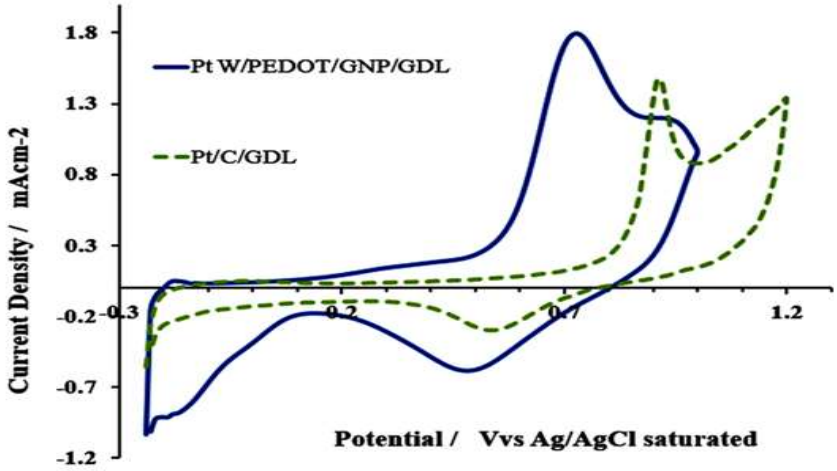

Fig. 16. CO stripping results for PtW/PEDOT/GNP/GDL and Pt/C/GDL catalysts in 0.5 M H_2SO_4 solution, scan rate:50 mVs^{-1}

GDL electrode is more tolerant to CO poisoning than the Pt/C/GDL electrode. One more interesting finding from the CO stripping study is related to the CO electro-oxidation onset potential, which can be further used to characterize the ease of CO oxidation. The onset and peak potential of CO on PtW/PEDOT/GNP/GDL (0.49V, 0.75V) is much lower than that of Pt/C/GDL (0.69V, 0.92V), respectively, which suggest that the PtW/PEDOT/GNP/GDL electrode has a higher CO oxidation ability and improved activity.

One more interesting finding is the difference between desorption area values of H^+ and CO in the prepared catalysts. The ESA values from H^+ adsorption and CO stripping areas are as follows: (ESACO=13.09, $ESAH^+$=14.48m^2g^{-1}) and (ESACO=5.63, $ESAH^+$= 35.37m^2g^{-1}) for PtW/PEDOT/GNP/GDL and Pt/C/GDL electrode, respectively.

3.8 Short term stability

Chronoamperometric experiments were performed to observe the stability and possible poisoning of the composite electrocatalyst under short periods of continuous operation in 0.5M H_2SO_4 +1M CH_3OH at 0.4V. As seen from Fig.17, the current density of the prepared PtW/PEDOT/GNP/GDL electrode and the commercial Pt/C/GDL decayed rapidly at the initial stage, which might be due to the formation of intermediate species, such as CO_{ads} and CH_{ads}, during methanol oxidation. The current gradually reached a relatively steady state after a brief transient period. It is clear from Fig.17 that the current density for the PtW/PEDOT/GNP/GDL electrode is much higher than that of the Pt/C/GDL in a longer time, indicating PEDOT electropolymerizied on a graphene support can improve the electrocatalytic activity and stability of the composite. These results again confirm the high tolerance to the intermediate species and superior electrocatalytic performance of the prepared PtW/PEDOT/GNP/GDL composite catalyst in MOR.

Also, the stability of each electrode was examined by cyclic voltammetry in N_2 saturated 0.5M H_2SO_4 .The potential sweep was from -0.24 to 1.2V vs Ag/AgCl (saturated) at 50mVs^{-1} . Fig. 18 a and b show the CV curves after continuous potential scanning obtained for Pt/C/GDL and PtW/PEDOT/GNP/GDL electrodes. As shown, the ECSA loss appeared on both catalysts under the potential cycling due to Pt dissolution or agglomeration. The results clearly revealed that the PtW/PEDOT/GNP/GDL electrode was more electrochemically stable than the Pt/C/GDL electrode.

4. Conclusion

The present study clearly demonstrated the potential of the PtW bimetallic alloy for use in methanol fuel cells. In this work several electrochemical process were used to foabricate Pt-based binary

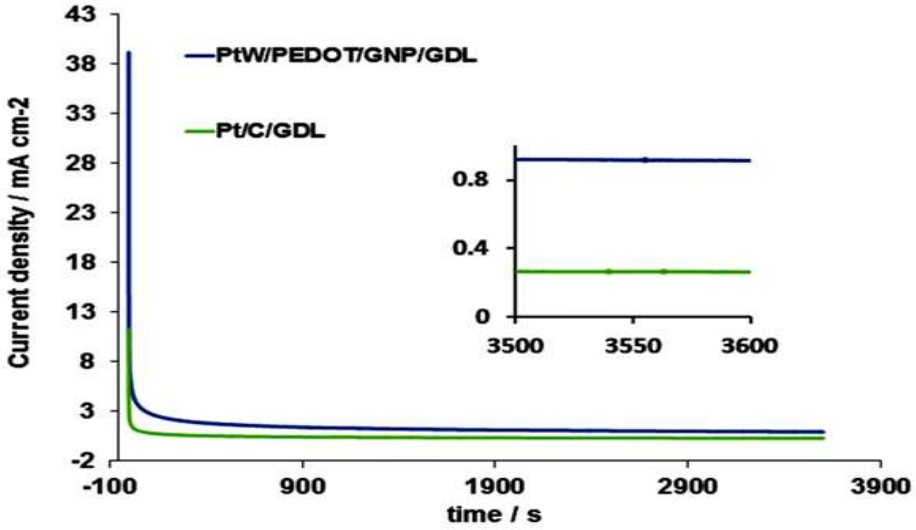

Fig. 17. Chronoamperometric curves of PtW/PEDOT/GNP/GDL and Pt/C/GDL catalysts in N_2 saturated aqueous solution of 0.5M H_2SO_4 containing 1M CH_3OH at fixed potential of 0.4V for 1h

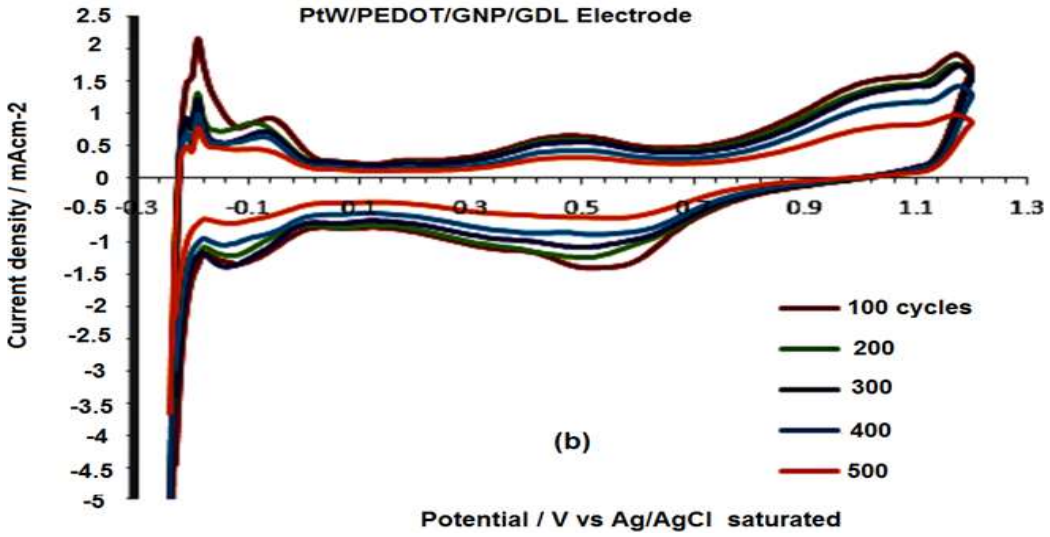

Fig. 18. CV of (a) Pt/C/GDL and (b) PtW/PEDOT/GNP/GDL electrodes in 0.5M H_2SO_4 solution scan rate:50 mVs^{-1}

alloys, polymerization of monomer, and reduction of support on gas diffusion layer to obtain a thin film with high activity for MOR. In the electrochemical measurements the PtW/PEDOT/GNP/GDL exhibited a higher CO electro-oxidation peak potential and much higher methanol electro-oxidation current density in comparison with that of Pt/C/GDL. Additionally, the PtW/PEDOT/GNP/GDL system showed good stability compared to the Pt/C/GDL electrode. These findings imply that PtW/PEDOT/GNP/GDL could be a very promising catalyst for anode applications with superior MOR activity and high CO tolerance in high–performance DMFCs.

Based on the electrochemical results it can be concluded that PEDOT covered graphene nanoplates possess a greater electrochemical activity than carbon used in Pt/C containing ink sprayed on carbon paper. Also, the results indicate a noticeable increase in the catalyst utilization due to the deposition of catalyst particles taking place only in the three-phase reaction zone. In conclusion, we present an effective and environmentally benign strategy to deposit electrocatalyst particles on GDL using an electrochemical method. The proposed technique could be very useful in the design and fabrication of DMFC electrodes.

Acknowledgement

This work was supported by New Technologies and the Hydrogen and Fuel cell Research Institute, Urmia University -Iran.

References

[1] Costamagna P. and Srinivasan S., "Quantum jumps in the PEMFC science and technology from the 1960s to the year 2000: Part II. Engineering, technology development and application aspects", J. Power Sources, 2001,102: 253.

[2] Carrette L., Friedrich K. and Stimming U., "Fuel cells–fundamentals and applications", Fuel cells, 2001,1: 5.

[3] Wang J., Wasmus S. and Savinell R., "Evaluation of Ethanol, 1-Propanol, and 2-Propanol in a Direct Oxidation Polymer-Electrolyte Fuel Cell A Real-Time Mass Spectrometry Study", J. Electrochem. Soc., 1995,142: 4218.

[4] Schmidt V.M., Ianniello R., Pastor E. and González S., "Electrochemical reactivity of ethanol on porous Pt and PtRu: Oxidation/reduction reactions in 1 M $HClO_4$", J. Phys. Chem., 1996, 100: 17901.

[5] Arico A., Srinivasan S. and Antonucci V., "DMFCs: from fundamental aspects to technology development", Fuel cells, 2001,1: 133.

[6] Vigier F., Coutanceau C., Perrard A., Belgsir E. and Lamy C., "Development of anode catalysts for a direct ethanol fuel cell", J. Appl. Electrochem., 2004,34: 439.

[7] Stamenkovic V.R., Fowler B., Mun B.S., Wang G., Ross P.N., Lucas C.A. and Marković N.M., "Improved oxygen reduction activity on Pt3Ni (111) via increased surface site availability", science, 2007,315: 493.

[8] Zhang J., Sasaki K., Sutter E. and Adzic R., "Stabilization of platinum oxygen-reduction electrocatalysts using gold clusters", Science, 2007,315: 220.

[9] Zhang J., Vukmirovic M.B., Xu Y., Mavrikakis M. and Adzic R.R., "Controlling the Catalytic Activity of Platinum-Monolayer Electrocatalysts for Oxygen Reduction with Different Substrates", Angew. Chem. Int. Ed., 2005,44: 2132.

[10] Chen Z., Waje M., Li W. and Yan Y., "Supportless Pt and PtPd Nanotubes as Electrocatalysts for Oxygen-Reduction Reactions", Angew. Chem. Int. Ed., 2007,46: 4060.

[11] Tian N., Zhou Z.-Y., Sun S.-G., Ding Y. and Wang Z.L., "Synthesis of tetrahexahedral platinum nanocrystals with high-index facets and high electro-oxidation activity", science, 2007,316: 732.

[12] Gong K., Du F., Xia Z., Durstock M. and Dai L., "Nitrogen-doped carbon nanotube arrays with high electrocatalytic activity for oxygen reduction", science, 2009,323: 760.

[13] Lim B., Jiang M., Camargo P.H., Cho E.C., Tao J., Lu X., Zhu Y. and Xia Y., "Pd-Pt bimetallic nanodendrites with high activity for oxygen reduction", science, 2009,324: 1302.

[14] He T. and Kreidler E., "Combinatorial screening of PtTiMe ternary alloys for oxygen electroreduction", Phys. Chem. Chem. Phys, 2008,10: 3731.

[15] Moore J.T., Chu D., Jiang R., Deluga G.A. and Lukehart C., "Synthesis and Characterization of Os and Pt− Os/Carbon Nanocomposites and their Relative Performance as Methanol Electrooxidation Catalysts", Chem. Mater., 2003,15: 1119.

[16] Park K.-W., Choi J.-H., Kwon B.-K., Lee S.-A., Sung Y.-E., Ha H.-Y., Hong S.-A., Kim H. and Wieckowski A., "Chemical and electronic effects of Ni in Pt/Ni and Pt/Ru/Ni alloy nanoparticles in methanol electrooxidation", J. Phys. Chem. B, 2002,106: 1869.

[17] Liu Z., Lee J.Y., Han M., Chen W. and Gan L.M., "Synthesis and characterization of PtRu/C catalysts

from microemulsions and emulsions", J. Mater. Chem., 2002,12: 2453.

[18] Boxall D.L., Kenik E.A. and Lukehart C., "Synthesis of PtSn/carbon nanocomposites using trans-PtCl (PEt3) 2 (SnCl3) as the source of metal", Chem. Mater., 2002,14: 1715.

[19] Steigerwalt E.S., Deluga G.A. and Lukehart C., "Pt− Ru/carbon fiber nanocomposites: synthesis, characterization, and performance as anode catalysts of direct methanol fuel cells. A search for exceptional performance", J. Phys. Chem. B, 2002,106: 760.

[20] Lee S.-A., Park K.-W., Choi J.-H., Kwon B.-K. and Sung Y.-E., "Nanoparticle synthesis and electrocatalytic activity of Pt alloys for direct methanol fuel cells", J. Electrochem. Soc., 2002,149: A1299.

[21] Götz M. and Wendt H., "Binary and ternary anode catalyst formulations including the elements W, Sn and Mo for PEMFCs operated on methanol or reformate gas", Electrochim. Acta, 1998,43: 3637.

[22] Zhou W., Zhou Z., Song S., Li W., Sun G., Tsiakaras P. and Xin Q., "Pt based anode catalysts for direct ethanol fuel cells", Appl.Catal.B., 2003,46: 273.

[23] Goetz M. and Wendt H., "Composite electrocatalysts for anodic methanol and methanol-reformate oxidation", J. Appl. Electrochem., 2001,31: 811.

[24] Christian J.B., Smith S.P., Whittingham M.S. and Abruña H.D., "Tungsten based electrocatalyst for fuel cell applications", Electrochem. Commun., 2007,9: 2128.

[25] Trogadas P. and Ramani V., "Pt⁄ C–WO3 Electrocatalysts for Degradation Mitigation in Polymer Electrolyte Fuel Cells", J. Electrochem. Soc., 2008,155: B696.

[26] Inzelt G., Pineri M., Schultze J. and Vorotyntsev M., "Electron and proton conducting polymers: recent developments and prospects", Electrochim. Acta, 2000,45: 2403.

[27] Inzelt G., "Conducting polymers: a new era in electrochemistry", Springer Science & Business Media. 2012.

[28] Kirchmeyer S., Elschner A., Reuter K., Lovenich W. and Merker U., "PEDOT as a conductive polymer: principles and applications", CRC Press New York, 2010.

[29] Heywang G. and Jonas F., "Poly (alkylenedioxythiophene) s—new, very stable conducting polymers", Adv. Mater., 1992,4: 116.

[30] Tsakova V., "How to affect number, size, and location of metal particles deposited in conducting polymer layers", J. Solid State Electrochem., 2008,12: 1421.

[31] Groenendaal L., Jonas F., Freitag D., Pielartzik H. and Reynolds J.R., "poly (3, 4-ethylenedioxythiophene) and its derivatives: past, present, and future", Adv. Mater., 2000,12: 481.

[32] Chen J., Jia C. and Wan Z., "Novel hybrid nanocomposite based on poly (3, 4-ethylenedioxythiophene)/multiwalled carbon nanotubes/graphene as electrode material for supercapacitor", Synth. Met., 2014,189: 69.

[33] Xu Y., Wang Y., Liang J., Huang Y., Ma Y., Wan X. and Chen Y., "A hybrid material of graphene and poly (3, 4-ethyldioxythiophene) with high conductivity, flexibility, and transparency", Nano Research, 2009,2: 343.

[34] Ying Wang C.-e.Z., Dong Sun,Jian-Rong Zhang and Jun-Jie Zhu, "A Graphene /Pol(3,4-ethylenedioxythiophene) Hybrid as a Anode for High –Performance Microbial Fuel Cells", chem plus chem, 2013,78: 823.

[35] Trang L.K.H., Thanh Tung T., Young Kim T., Yang W.S., Kim H. and Suh K.S., "Preparation and characterization of graphene composites with conducting polymers", Polymer International, 2012,61: 93.

[36] Lota K., Khomenko V. and Frackowiak E., "Capacitance properties of poly (3, 4-ethylenedioxythiophene)/carbon

nanotubescomposites", J. Phys. Chem. Solids, 2004,65: 295.

[37] Chen L., Yuan C., Dou H., Gao B., Chen S. and Zhang X., "Synthesis and electrochemical capacitance of core–shell poly (3, 4-ethylenedioxythiophene)/poly (sodium 4-styrenesulfonate)-modified multiwalled carbon nanotube nanocomposites", Electrochim. Acta, 2009,54: 2335.

[38] Chu C.-Y., Tsai J.-T. and Sun C.-L., "Synthesis of PEDOT-modified graphene composite materials as flexible electrodes for energy storage and conversion applications", Int. J. Hydrogen Energy, 2012,37: 13880.

[39] Yaldagard M., Seghatoleslami N. and Jahanshahi M., "Preparation of Pt-Co nanoparticles by galvanostatic pulse electrochemical codeposition on in situ electrochemical reduced graphene nanoplates based carbon paper electrode for oxygen reduction reaction in proton exchange membrane fuel cell", Appl. Surf. Sci., 2014,315: 222.

[40] Patra S. and Munichandraiah N., "Electrooxidation of methanol on Pt-modified conductive polymer PEDOT", Langmuir, 2008,25: 1732.

[41] Sakmeche N., Aeiyach S., Aaron J.-J., Jouini M., Lacroix J.C. and Lacaze P.-C., "Improvement of the electrosynthesis and physicochemical properties of poly (3, 4-ethylenedioxythiophene) using a sodium dodecyl sulfate micellar aqueous medium", Langmuir, 1999,15: 2566.

[42] Kudoh Y., Akami K. and Matsuya Y., "Chemical polymerization of 3, 4-ethylenedioxythiophene using an aqueous medium containing an anionic surfactant", Synth. Met., 1998,98: 65.

[43] Bazzaoui E., Aeiyach S. and Lacaze P., "Electropolymerization of bithiophene on Pt and Fe electrodes in an aqueous sodium dodecylsulfate (SDS) micellar medium", Synth. Met., 1996,83: 159.

[44] Hummers Jr W.S. and Offeman R.E., "Preparation of graphitic oxide", J.Am. Chem. Soc., 1958,80: 1339.

[45] Wang G., Shen X., Wang B., Yao J. and Park J., "Synthesis and characterisation of hydrophilic and organophilic graphene nanosheets", Carbon, 2009,47: 1359.

[46] Schrebler R., Grez P., Cury P., Veas C., Merino M., Gómez H., Cordova R. and Del Valle M., "Nucleation and growth mechanisms of poly (thiophene) Part 1. Effect of electrolyte and monomer concentration in dichloromethane", J. Electroanal. Chem., 1997,430: 77.

[47] Randriamahazaka H., Noel V. and Chevrot C., "Nucleation and growth of poly (3, 4-ethylenedioxythiophene) in acetonitrile on platinum under potentiostatic conditions", J. Electroanal. Chem., 1999,472: 103.

[48] Mo D., Zhou W., Ma X., Xu J., Zhu D. and Lu B., "Electrochemical synthesis and capacitance properties of a novel poly (3, 4-ethylenedioxythiophene bis-substituted bithiophene) electrode material", Electrochim. Acta, 2014,132: 67.

[49] Conway B.E., "Electrochemical supercapacitors: scientific fundamentals and technological applications", Springer Science & Business Media. 2013.

[50] Si P., Ding S., Lou X.-W.D. and Kim D.-H., "An electrochemically formed three-dimensional structure of polypyrrole/graphene nanoplatelets for high-performance supercapacitors", Rsc Advances, 2011,1: 1271.

[51] Han M.G. and Foulger S.H., "1-Dimensional structures of poly (3, 4-ethylenedioxythiophene) (PEDOT): a chemical route to tubes, rods, thimbles, and belts", Chem. Commun., 2005: 3092.

[52] Nie G., Qu L., Xu J. and Zhang S., "Electrosyntheses and characterizations of a new soluble conducting copolymer of 5-cyanoindole and 3, 4-ethylenedioxythiophene", Electrochim. Acta, 2008,53: 8351.

[53] Zhao-yang Z., Yi-jie T., Xiao-qian X., Yong-jiang Z., Hai-feng C. and Wen-wei Z., "Electrosynthesises and

characterizations of copolymers based on thiophene and 3, 4-ethylenedioxythiophene in boron trifluoride diethyl etherate", Synth. Met., 2012,162: 2176.

[54] Ma Y., Zhao F. and Zeng B., "Electrodeposition of poly (3, 4-ethylenedioxythiophene) on a stainless steel wire for solid phase microextraction and GC determination of some esters with high boiling points", Talanta, 2013,104: 27.

[55] Sarac A., Sönmez G. and Cebeci F., "Electrochemical synthesis and structural studies of polypyrroles, poly (3, 4-ethylene-dioxythiophene) s and copolymers of pyrrole and 3, 4-ethylenedioxythiophene on carbon fibre microelectrodes", J. Appl. Electrochem., 2003,33: 295.

[56] Lee C., Wei X., Kysar J.W. and Hone J., "Measurement of the elastic properties and intrinsic strength of monolayer graphene", science, 2008,321: 385.

[57] Kvarnström C., Neugebauer H., Blomquist S., Ahonen H., Kankare J. and Ivaska A., "In situ spectroelectrochemical characterization of poly (3, 4-ethylenedioxythiophene)", Electrochim. Acta, 1999,44: 2739.

[58] Wang X. and Wong K., "Effects of a base coating used for electropolymerization of poly (3, 4-ethylenedioxythiophene) on indium tin oxide electrode", Thin Solid Films, 2006,515: 1573.

[59] Ouyang J., Chu C.W., Chen F.C., Xu Q. and Yang Y., "High-conductivity poly (3, 4-ethylenedioxythiophene): poly (styrene sulfonate) film and its application in polymer optoelectronic devices", Adv. Funct. Mater., 2005,15: 203.

[60] Beard B.C. and Ross P.N., "The Structure and Activity of Pt-Co Alloys as Oxygen Reduction Electrocatalysts", J. Electrochem. Soc., 1990,137: 3368.

[61] Trasatti S. and Petrii O., "Real surface area measurements in electrochemistry", Pure Appl. Chem., 1991,63: 711.

[62] Beden B., Lamy C., De Tacconi N. and Arvia A., "The electrooxidation of CO: a test reaction in electrocatalysis", Electrochim. Acta, 1990,35: 691.

[63] Huang Q., Yang H., Tang Y., Lu T. and Akins D.L., "Carbon-supported Pt–Co alloy nanoparticles for oxygen reduction reaction", Electrochem. Commun., 2006,8: 1220.

[64] Cao L., Scheiba F., Roth C., Schweiger F., Cremers C., Stimming U., Fuess H., Chen L., Zhu W. and Qiu X., "Novel Nanocomposite Pt/RuO_2 x H_2O/Carbon Nanotube Catalysts for Direct Methanol Fuel Cells", Angew. Chem. Int. Ed., 2006,45: 5315.

[65] Cui G., Zhi L., Thomas A., Kolb U., Lieberwirth I. and Müllen K., "One-Dimensional Porous Carbon/Platinum Composites for Nanoscale Electrodes", Angewandte Chemie, 2007,119: 3534.

[66] Honda K., Yoshimura M., Rao T.N., Tryk D., Fujishima A., Yasui K., Sakamoto Y., Nishio K. and Masuda H., "Electrochemical properties of Pt-modified nano-honeycomb diamond electrodes", J. Electroanal. Chem., 2001,514: 35.

[67] Yaldagard M., Jahanshahi M. and Seghatoleslami N., "Pt catalysts on PANI coated WC/C nanocomposites for methanol electro-oxidation and oxygen electro-reduction in DMFC", Appl. Surf. Sci., 2014,317: 496.